Pediatr Radiol (2010) 40:326–339
DOI 10.1007/s00247-009-1504-2

PICTORIAL ESSAY

The dentate nucleus in children: normal development and patterns of disease

Aoife McErlean · Khaled Abdalla · Veronica Donoghue · Stephanie Ryan

Received: 17 April 2009 / Revised: 17 November 2009 / Accepted: 22 November 2009 / Published online: 28 January 2010

Abstract The dentate nuclei lie deep within the cerebellum and play a vital role in the pathways involved in fine motor control and coordination. They are susceptible to a variety of diseases. Some pathological processes preferentially affect the dentate nuclei, while concomitant basal ganglia or white matter involvement can be a striking finding in others. A familiarity with the normal appearance of the dentate nuclei at different ages in combination with the radiological distribution of pathology in the brain allows the paediatric radiologist to develop a logical approach to the interpretation of MR imaging of these deep cerebellar nuclei. In this article we review the normal appearance and MR features of the dentate nuclei, including changes that are seen with myelination. We describe the specific imaging characteristics of childhood diseases that involve the dentate nuclei, and develop a systematic approach to the differential diagnosis of dentate nucleus abnormalities on MR imaging.

Keywords Cerebellar nuclei · MRI · Anatomy · Cross-sectional · Paediatrics · Cerebellum · Dentate

Introduction

The dentate nucleus is the largest and most lateral of the deep cerebellar nuclei. Named because of its toothed appearance, the dentate forms part of the functional neo-cerebellum, which is involved in the coordination and timing of fine and skilled voluntary movements including speaking, writing and dancing. It receives its afferents from the premotor cortex and the supplementary motor cortex via the pontocerebellar system. Efferent fibres from the dentate nucleus pass in the superior cerebellar peduncles and cross over at the pontomesencephalic junction to synapse in the red nucleus, then on to the ventrolateral thalamus and project to the motor cortex (Fig. 1).

A variety of disease processes can affect the dentate nuclei; some preferentially involve the dentate nucleus, while others are associated with basal ganglia and white matter changes. Familiarity with the normal appearance of the dentate nuclei at different ages, combined with the radiological distribution of pathology in the brain, suggests a differential diagnosis in children with MR abnormalities identified in these deep cerebellar nuclei.

MR imaging parameters

MR imaging was performed on a 1.5-T Signa system (General Electric, Milwaukee, Wis.). The MR imaging protocols used in our department included the following sequences and parameters: axial T1-weighted (T1-W) spin-echo (neonates to 6 months TR 500 ms, TE 9 ms; >6 months TR 405 ms TE 9 ms), axial T2-weighted (T2-W) fast spin-echo (neonates TR 4,525 ms, TE 200 ms; 3–6 months TR 4,000 ms, TE 140 ms; >6 months TR 4,050 ms, TE 85 ms), T2 FLAIR (TR 9,000 ms, TI 2,200 ms, TE 120 ms) and T1-W inversion recovery (TR 2,000 ms, TI 750 ms, TE 9 ms).

MR appearance of the normal dentate nucleus

The normal appearance of the dentate changes as myelination progresses in the first years of life [1]. We have

A. McErlean (✉) · K. Abdalla · V. Donoghue · S. Ryan
Radiology Department, Children's University Hospital,
Temple Street,
Dublin 1, Ireland
e-mail: aoife@mcerlean.cc

Fig. 1 Connections of the dentate nucleus. (*scp* superior cerebellar peduncle, 1 dentate nucleus, 2 red nucleus, 3 thalamus, 4 motor cortex, 5 pontine nuclei, 6 neocerebellum)

reviewed a large number of normal MRI scans at various ages and can describe the following findings.

T1-W MR

At term the normal dentate nucleus on T1-W images is hypointense to adjacent myelinated white matter (Fig. 2). As myelination progresses both the central part of the dentate and the peridentate white matter become brighter on T1-W images by the third month of life [2]. The dentate nucleus becomes difficult to distinguish from the surrounding cerebellar peduncles on T1 images by 6 months. Hyperintensity of the central part of the dentate compared with surrounding white matter is always abnormal.

T2-W MR

At term the normal dentate nuclei are hyperintense on T2-W MR with a dark outer serrated border [1]. Over the first year the central part of the dentate nuclei becomes isointense with grey matter, while the outer border blends with gradually myelinating middle cerebellar peduncles and the white matter of the cerebellum. By 2 years of age the dentate nuclei become difficult to distinguish from the medial borders of the adjacent cerebellar white matter (Fig. 3).

Diffusion-weighted imaging (DWI)

The normal dentate nuclei are not distinguishable from surrounding white matter on DWI. On apparent diffusion coefficient (ADC) images in the first 6 months of life the normal dentate may be detectable by very slightly less restricted diffusion than adjacent white matter (Fig. 4). Brightness of the dentate on DWI and significant hypointensity on ADC images is therefore always abnormal.

The dentate and disease

A wide variety of pathological processes can involve the dentate nuclei including metabolic, genetic and neurodegenerative disorders, ischaemia and some infections. In the next section we will review the salient imaging features that have been observed when the dentate nucleus is involved in these diseases.

Metabolic disorders

Mitochondrial disorders is a collective term for a wide variety of overlapping conditions involving defects in the

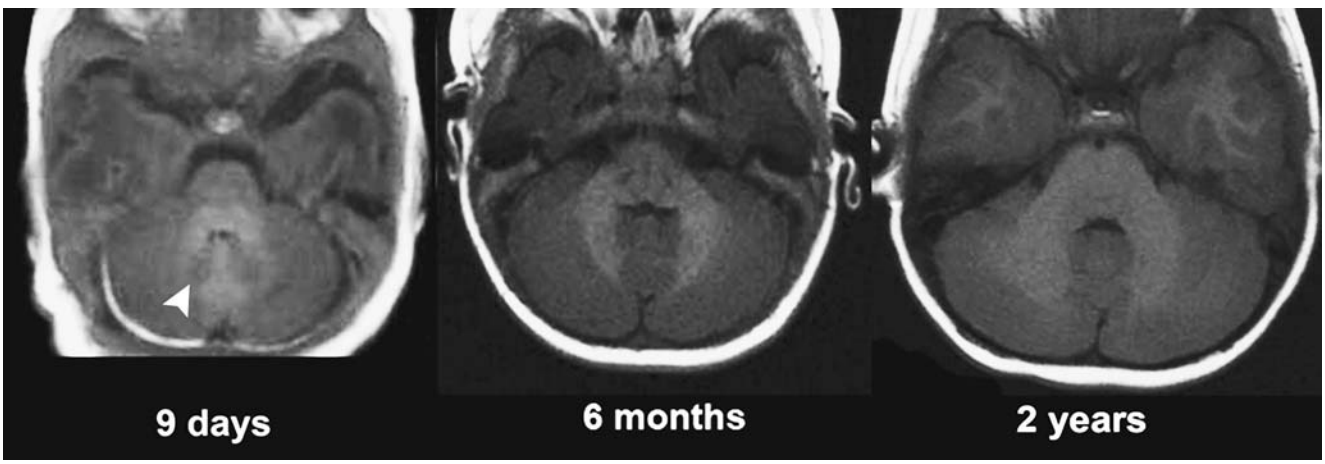

Fig. 2 Normal appearance of the dentate nucleus on T1-W imaging. The hypointense dentate nuclei are easily distinguishable in the first few days of life (*arrowheads*) but by 6 months myelination within the dentate nuclei make them difficult to distinguish from the surrounding white matter

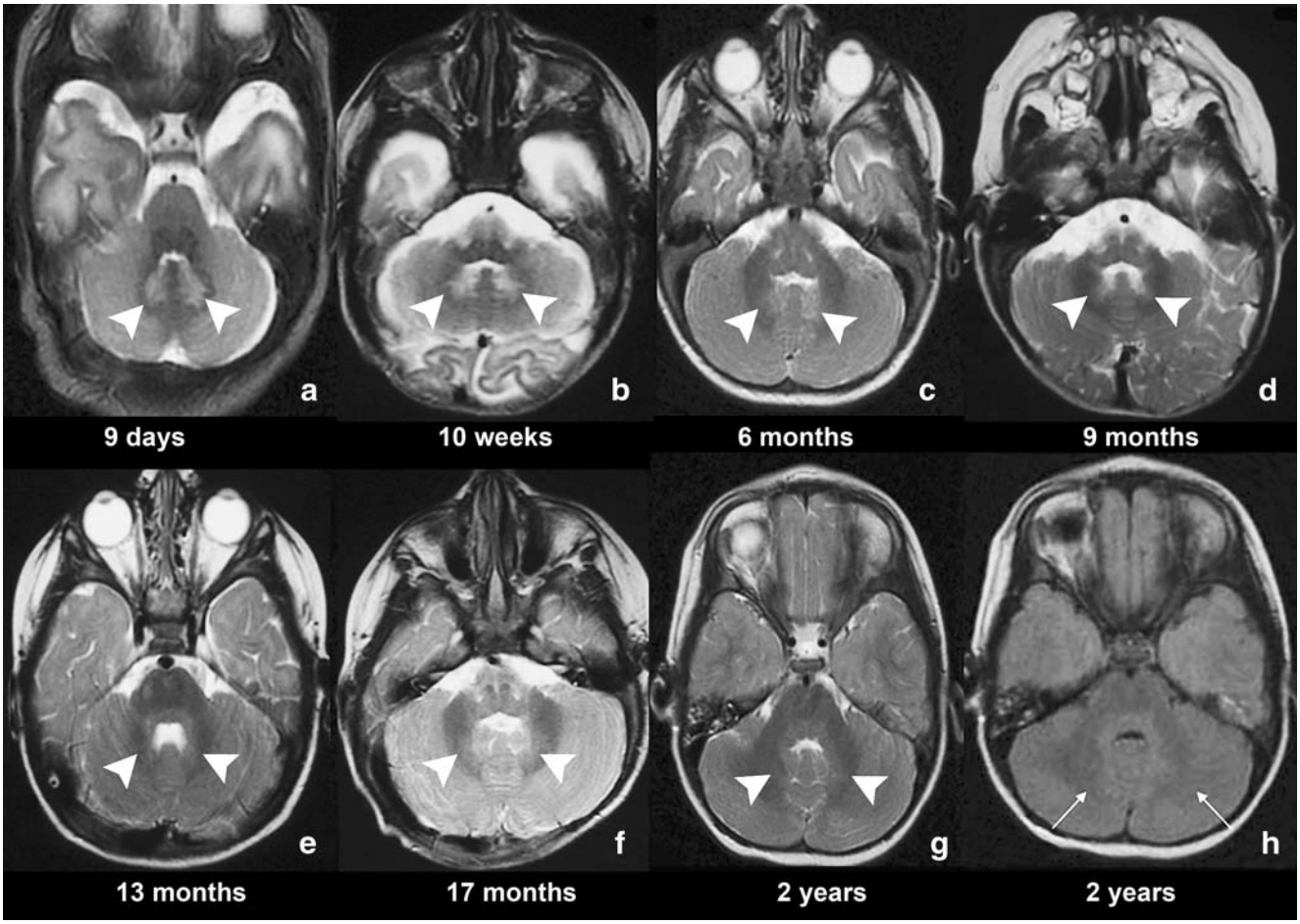

Fig. 3 Normal appearance of the dentate nucleus. **a–g** Axial T2-W imaging from birth to year 2 of life shows the dentate nuclei (*arrowheads*). **h** FLAIR image in a 2-year-old child. The dentate nucleus remains somewhat distinguishable from the peridentate white matter (*arrows*)

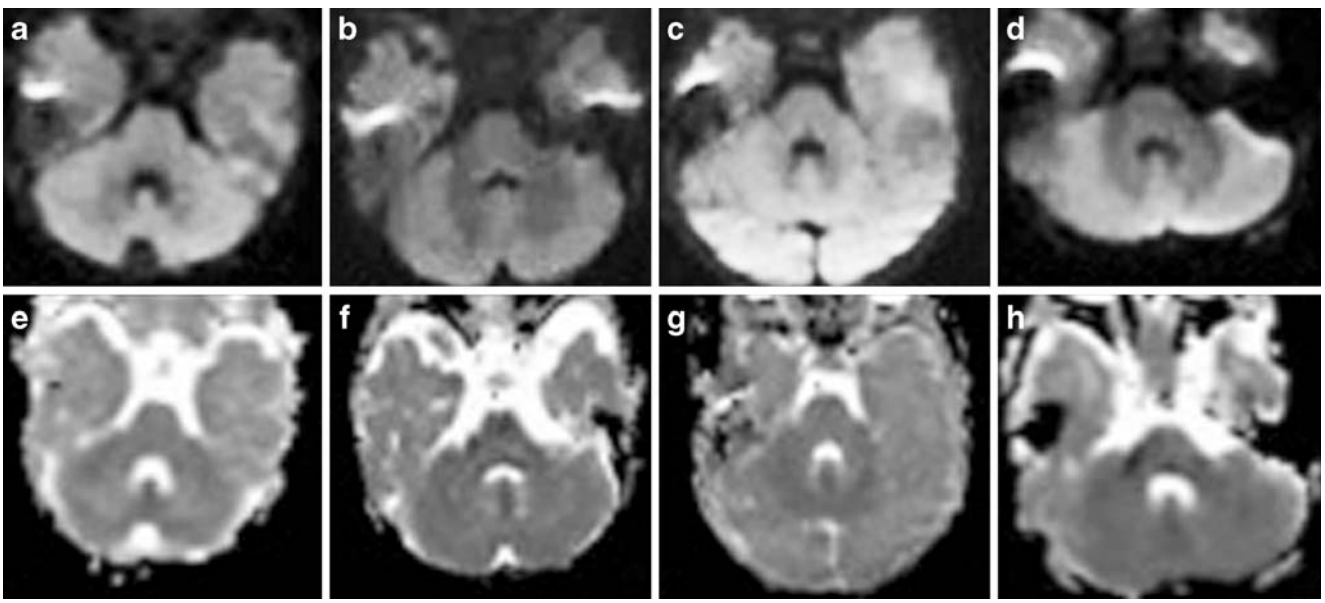

Fig. 4 DWI images at (**a**) 12 days, (**b**) 3 months (**c**) 6 months and (**d**) 1 year of age show that normal dentate is not distinguishable from surrounding white matter. On corresponding ADC images at (**e**) 12 days, (**f**) 3 months (**g**) 6 months and (**h**) 1 year of age the normal dentate may be detectable by very slightly less restricted diffusion than adjacent white matter

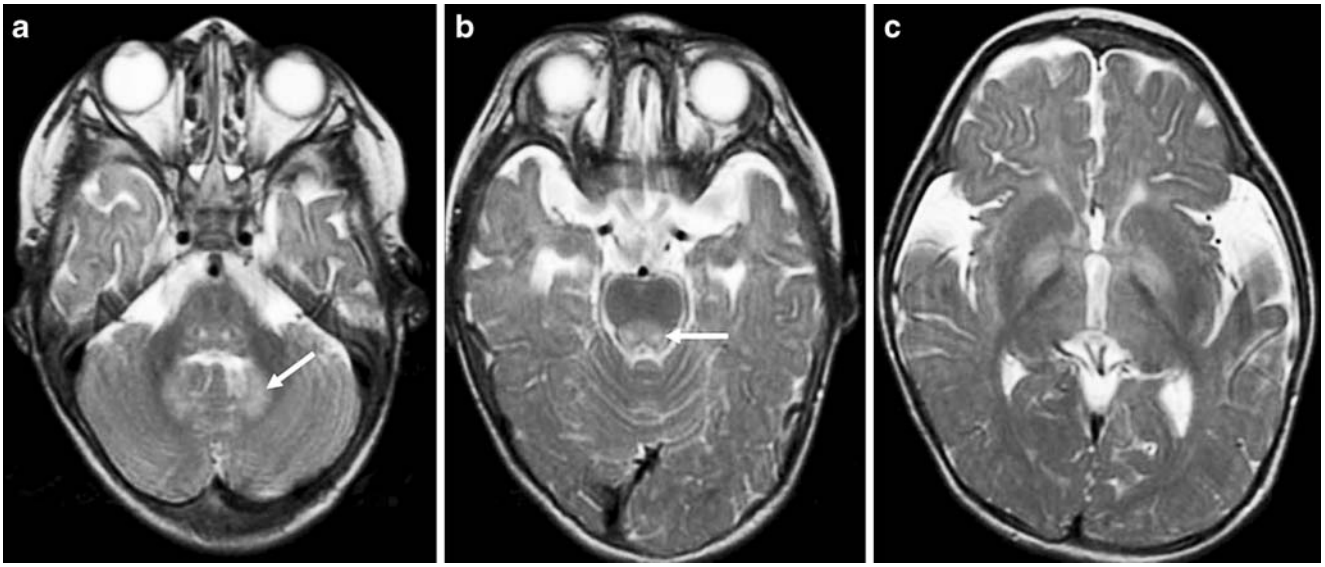

Fig. 5 An 11-month-old girl with Leigh disease (complex I and V deficiency). Axial T2-W imaging. There is hyper-intense signal in (**a**) the dentate nucleus (*arrow*) and medial lemnisci in the posterior pons, (**b**) the medial lemnisci in the posterior midbrain (*arrow*) and (**c**) the globi palladi

respiratory chain; a complex multiunit system within the inner membrane of mitochondria involved in the process of oxidative phosphorylation. Mitochondrial disorders exhibit a broad spectrum of clinical manifestations, imaging features and inheritance patterns. There is often overlap between different disease entities with regards to both clinical and imaging features [3, 4].

Leigh disease (subacute necrotising encephalomyelopathy) refers to a symptom complex with characteristic but variable clinical and pathological manifestations, which usually presents in the first year of life with psychomotor retardation and brain stem dysfunction. There is progressive neurological deterioration with lactic acidaemia. Several biochemical and genetic abnormalities cause Leigh disease. However four main groups of defects appear to be responsible for the majority of cases—defect of pyruvate dehydrogenase complex, cytochrome oxidase (COX, complex IV), complex V and complex I deficiencies [5]. On T2-W and fluid-attenuated inversion recovery (FLAIR) sequences, focal high-signal intensities, which are often bilaterally symmetric, can be seen in the peri-aqueductal grey matter, the remainder of the brain stem, basal ganglia, thalami, subthalamic and dentate nuclei (Fig. 5) [3–7].

Glutaric aciduria type 1 (GA1), an autosomal-recessive (AR) inborn error of metabolism, is due to mitochondrial glutaryl-co-enzyme A dehydrogenase deficiency. This is

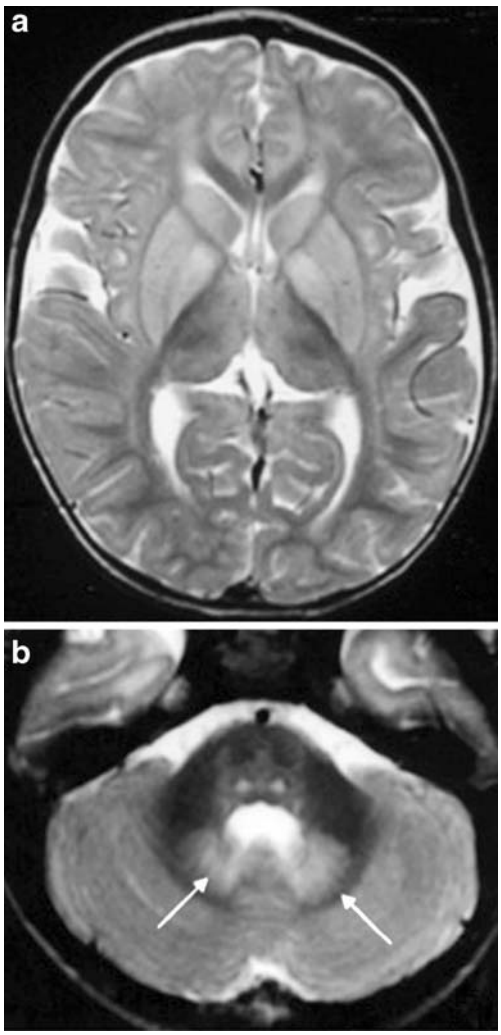

Fig. 6 An 18-month-old girl with GA1. **a** Axial T2-W images through the cerebrum at the level of the basal ganglia shows high signal in the lentiform and caudate nuclei. Abnormal mixed signal is also seen in the thalami. **b** The dentate nuclei demonstrate abnormal high signal (*arrows*). The medial lemnisci in the posterior pons also have abnormal increased signal intensity

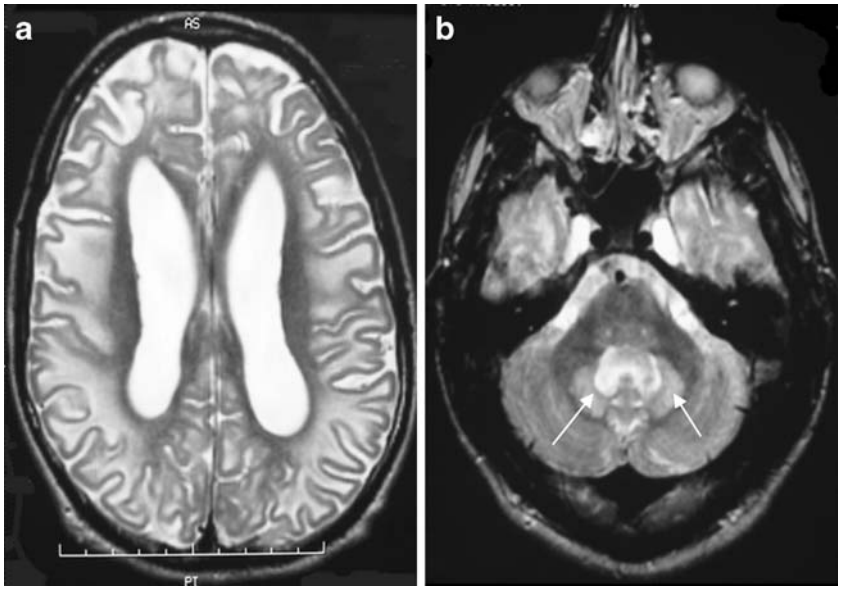

Fig. 7 A 22-year-old man (who presented in childhood) with L-2 hydroxyglutaric aciduria. Axial T2-W images. **a** Image demonstrates high signal abnormality and swelling affecting the superficial cerebral white matter and sub-cortical U-fibres. There is relative sparing of the deep white matter. **b** Abnormal high signal is shown in the dentate nuclei bilaterally (*arrows*)

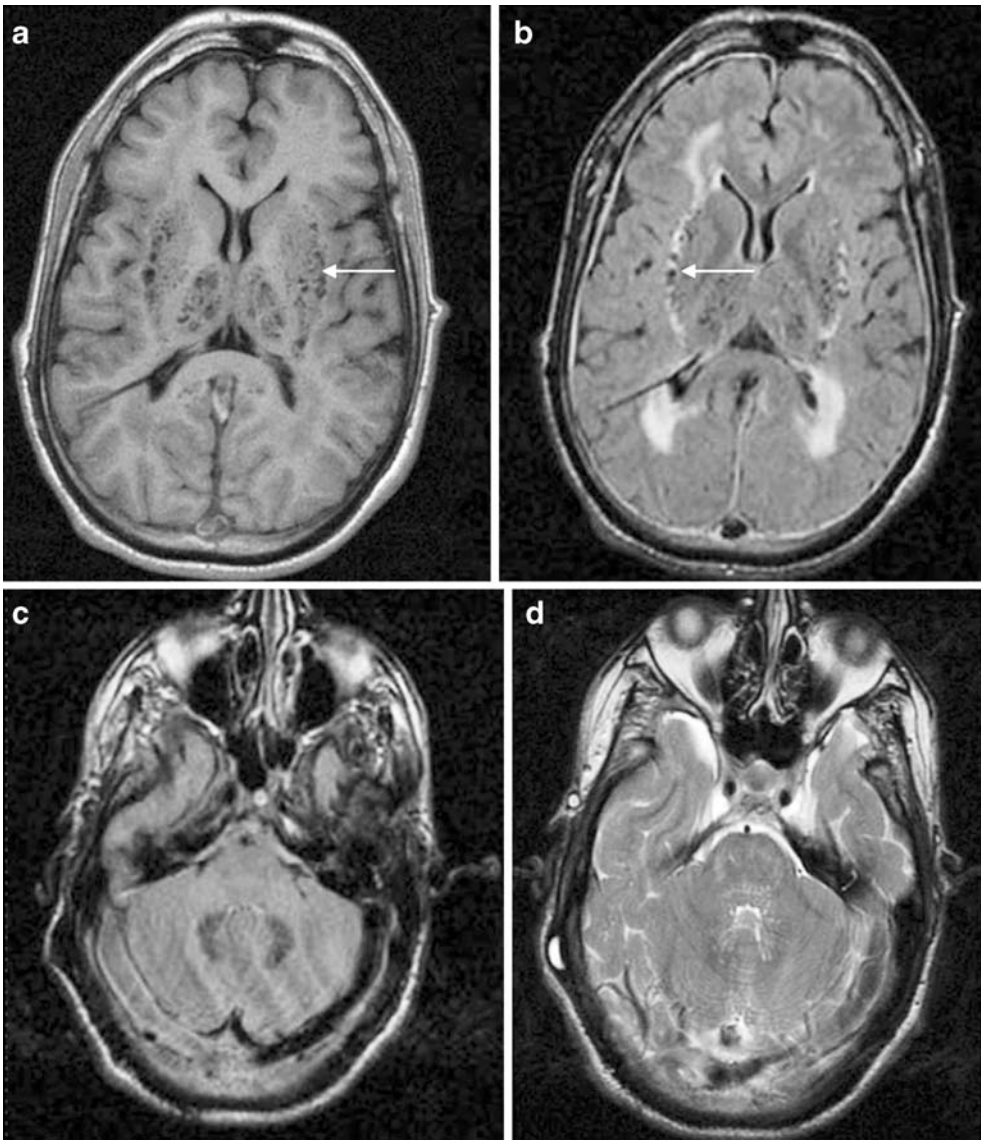

Fig. 8 An 18-year-old child with MPS 1, Hurler –Scheie phenotype. **a** Axial T1-W image showing cyst-like lesions within basal ganglia, thalami and external capsule (*arrow*). **b** T2 FLAIR image shows abnormal white matter signal. There is also cyst formation in the external capsules (*arrow*). **c** The dentate has low signal on T2 FLAIR and (**d**) mixed signal on T2-W images

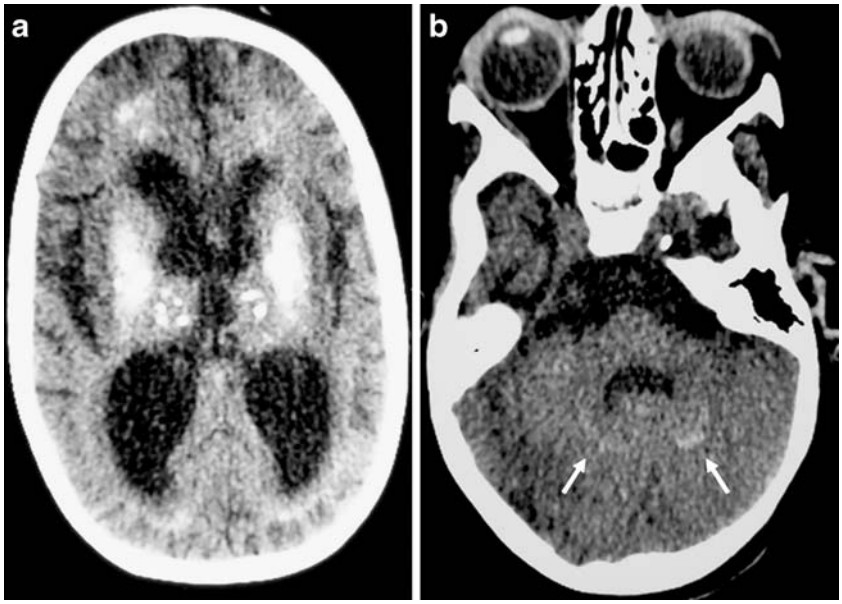

Fig. 9 Non-contrast CT brain in a 3-year-old boy with Aicardi-Goutieres syndrome. **a** Calcification is seen in the basal ganglia, both thalami and the white matter of both frontal lobes and (**b**) in the dentate nuclei (*arrows*)

not a respiratory chain disorder but an organic aciduria. It is characterized clinically by episodic acute encephalopathic crises. Frontotemporal atrophy and dilatation of the sylvian fissures is seen on MR imaging in 93% of GA1 patients. Signal abnormalities in the basal ganglia progress to atrophy over time (Fig. 6). Other findings in GA1 include white matter and dentate nuclei abnormalities (Fig. 6) and reduced NAA peak on MR spectroscopy (MRS) [8]. Elevated lactate on MRS may be seen during a crisis [9].

L-2 hydroxyglutaric aciduria is an AR organic aciduria of unknown aetiology. As the clinical presentation is often non-specific, the distinctive MR brain appearance of this disorder can be key in initiating the appropriate metabolic workup. Both grey and white matter are involved. The white matter changes follow a centripetal distribution with the subcortical U-fibres being the most severely affected (Fig. 7). The basal ganglia and dentate nuclei are always abnormal and are often swollen (Fig. 7). Gradual cerebral and cerebellar atrophy develop over time with progression of disease [10, 11].

Mucopolysaccharidoses (MPS) are inherited disorders of metabolism characterised by enzyme deficiency that results in inability to break down glycosaminoglycan. MPS are classified according to the specific enzyme deficiency. The perivascular (Virchow-Robin) spaces

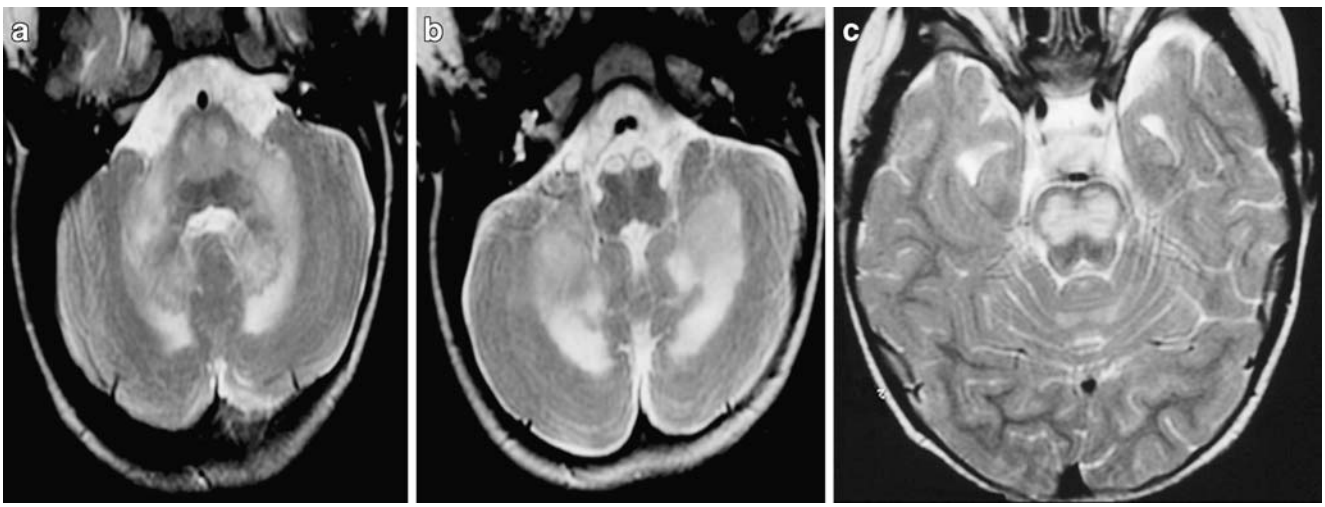

Fig. 10 A 2-year-old boy with straight-chain acyl-CoA oxidase deficiency. **a–c** Axial T2-W images through the cerebellum demonstrate abnormal high signal in the dentate nuclei, cerebellar white matter and in the pons and midbrain

become dilated by accumulated glycosaminoglycan producing a cribriform appearance of the white matter (Fig. 8), corpus callosum and basal ganglia on MRI. The dentate nuclei can demonstrate abnormal signal (Fig. 8). Other neuroimaging features seen in MPS include craniocervical junction compression and occasional arachnoid cysts [12].

Aicardi-Goutieres syndrome Aicardi and Goutieres [13] in 1984 reported eight cases of progressive familial encephalopathy in infancy, with basal ganglia calcification and chronic cerebrospinal fluid lymphocytosis. There was rapid deterioration to a vegetative state [13]. Aicardi-Goutieres syndrome is an AR disorder and is phenotypically similar to in-utero viral infection. There is cerebral atrophy, white matter abnormality and cerebral calcification (Fig. 9). Dentate nuclei may be affected [14].

Peroxisomal disorders are subdivided into two major categories. Peroxisome biogenesis disorders are disorders resulting from a failure to form normal peroxisomes, resulting in multiple metabolic abnormalities. The second category includes those disorders resulting from the deficiency of a single peroxisomal enzyme. The dentate nucleus may be affected in both types of peroxisomal disorders including infantile Refsum disease, X-linked adrenoleukodystrophy and acyl CoA oxidase deficiency (Fig. 10) [15].

Maple syrup urine disease (MSUD) is an inherited disorder of branched chain amino acid metabolism presenting in newborns with neurological deterioration, ketoacidosis and hyper-ammonemia. There is marked fluid restriction seen in DWI with reduced ADC map signal in keeping with myelin oedema. The oedema usually involves the cerebellum including the dentate nuclei, the brain stem and corticospinal tracts more than the cerebral hemispheres (Fig. 11) [16, 17].

White matter diseases

Canavan disease is a progressive AR leukodystrophy due to aspartoacyclase deficiency resulting in N-acetyl aspartic aciduria. MR imaging reveals diffuse symmetric cerebral white matter abnormalities with low T1-W and high T2-W signal intensity. There is early preferential involvement of the subcortical white matter, thalami and globus palladi. Deep white matter and dentate nuclei abnormalities occur later [10]. Distinctive elevation of N-acetyl-aspartate (NAA) is visible on MRS (Fig. 12).

Globoid cell leukodystrophy (Krabbe disease) is a progressive AR degenerative leukodystrophy due to a deficiency of galactocerebroside beta-galactosidase. In the very early stages MR imaging can be normal but CT may demonstrate hyperdense basal ganglia, thalami and dentate nuclei. As the disease develops the deep cerebral white matter becomes hypointense on T1-W and hyperintense on T2-W sequences. Abnormal signal is also seen in the basal ganglia and thalami as well as the dentate nuclei (Fig. 13) [18, 19].

Megalencephalic leukoencephalopathy with cysts (previously known as Van Der Knaap leukoencephalopathy) is an autosomal-recessive neurodegenerative leukoencephalopathy. Affected children have macrocephaly from birth or develop it in the first year of life. There is usually mild developmental delay and cerebellar ataxia develops early in childhood. By their teens, MR of the brain shows swollen white matter with sub-cortical cysts especially anterior temporal and fronto-parietal regions (Fig. 14). Dentate nucleus involvement has been described (Fig. 14) [20].

Merosin-negative muscular dystrophy comprises only 30% of congenital muscular dystrophies. This heterogeneous group of AR myopathies present at birth with hypotonia. There is significant hypomyelination and high

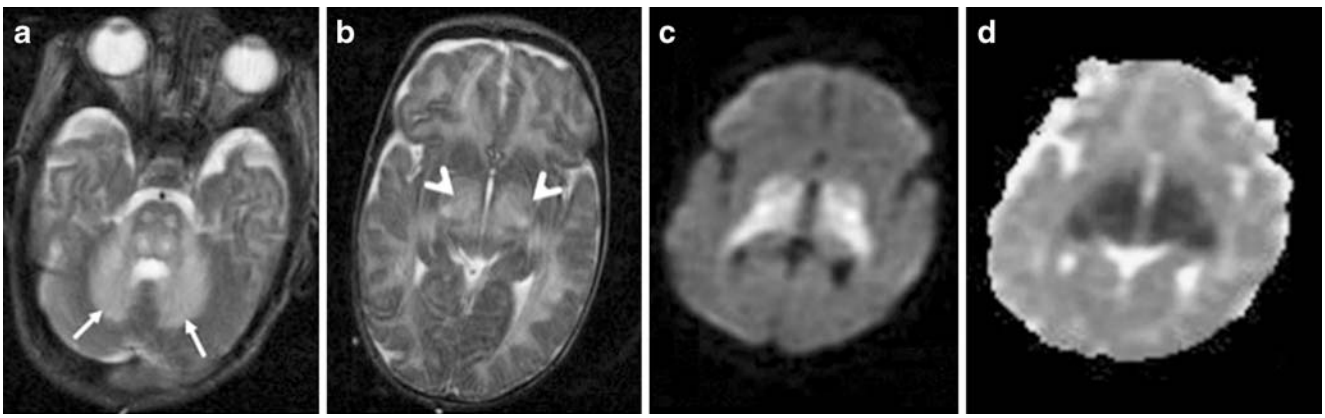

Fig. 11 A 1-month-old infant girl with MSUD. **a, b** Axial T2-W images through the cerebellum and at sylvian fissure level show hyperintensity in (**a**) both dentate nuclei (*white arrows*) and cerebellar white matter, (**b**) the thalami (*arrowheads*) and white matter. **c** DWI through the basal ganglia shows abnormal hyperintensity in both thalami, globi pallidi and posterior limb of internal capsule. **d** ADC confirms restricted diffusion in the same areas in keeping with myelin oedema

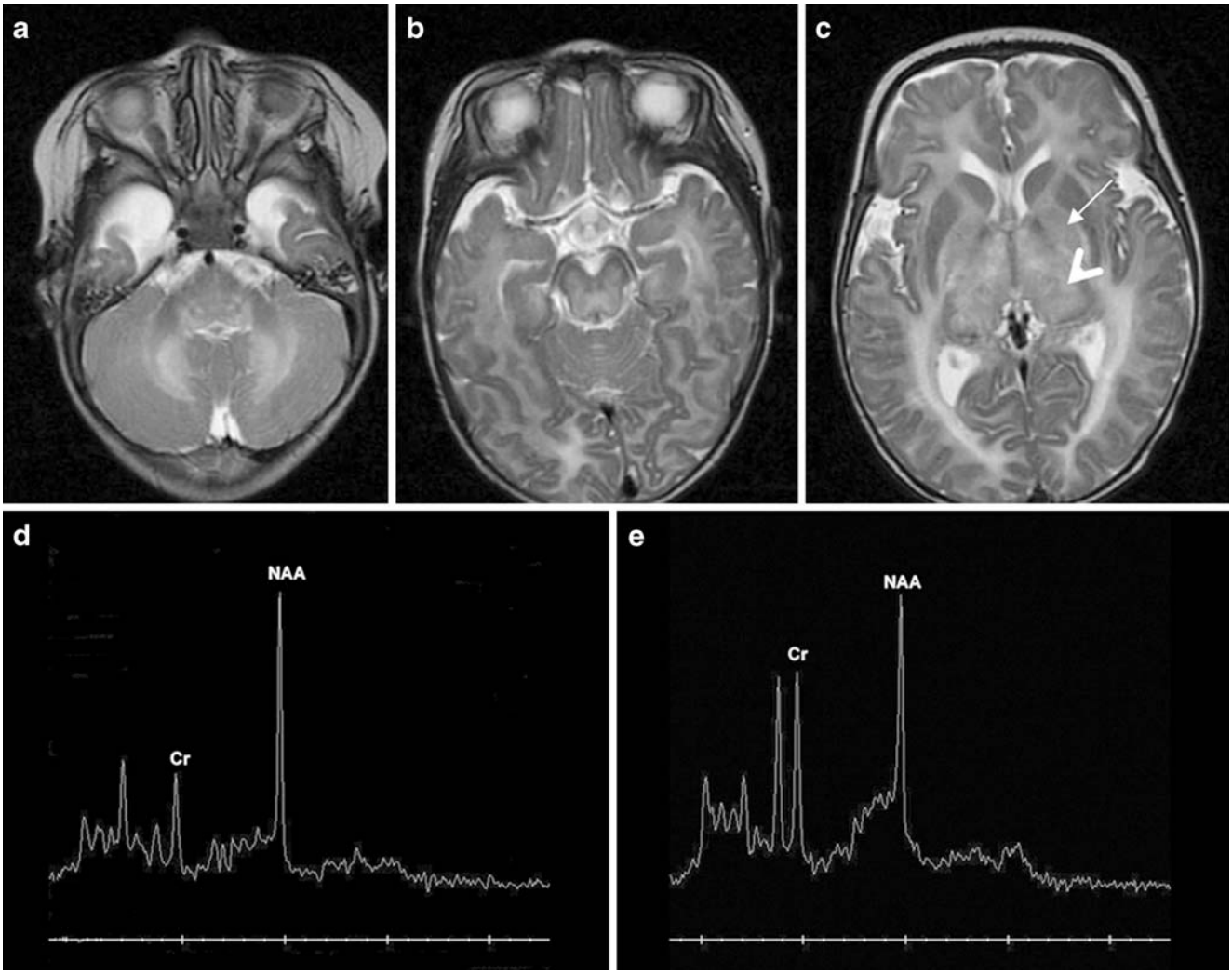

Fig. 12 A 6-month-old girl with Canavan disease. **a–c** T2-W imaging shows hyperintensities in the cerebellar white matter, dentate nuclei, brain stem, thalami (*arrowhead*) and globi pallidi (*arrow*). **d** MRS (centered on left thalamus and adjacent lentiform nucleus, TE 35 ms) shows marked NAA peak. **e** Normal MRS in this location at the same age. Note how the NAA peak is 1.5 times higher than the creatine (Cr) peak, compared with three times higher in the child with Canavan disease

T2 signal of white matter in the merosin-negative type. High signal may also be seen in the dentate nuclei and in the cerebellar white matter (Fig. 15). Additional MRI findings include polymicrogyria and callosal, vermian or septal hypogenesis [21].

Miscellaneous disorders

In the preceding few sections we have described the abnormal MR appearance of the dentate nuclei in a variety of rare genetic and metabolic disorders. We have also observed dentate nuclei abnormalities in more commonly encountered childhood diseases including ischaemic insults and infection, phakomatoses and Langerhans cell histiocytosis (LCH).

Ischaemia

Particular susceptibility of the dentate nuclei to ischaemia has not been described but we have found that the dentate nuclei may be particularly involved in diffuse acute ischaemia while other posterior fossa structures are relatively spared (Fig. 16). The dentate nuclei are supplied by the superior cerebellar artery but selective involvement cannot be explained by vascular distribution and is more likely related to a high metabolic rate comparable to that seen in the thalami and basal ganglia.

We have also seen unilateral changes in the dentate nuclei associated with prior contralateral cerebral ischaemia (Fig. 16). This is a form of crossed cerebellar diaschisis. Predominant involvement of the dentate in diaschisis has not

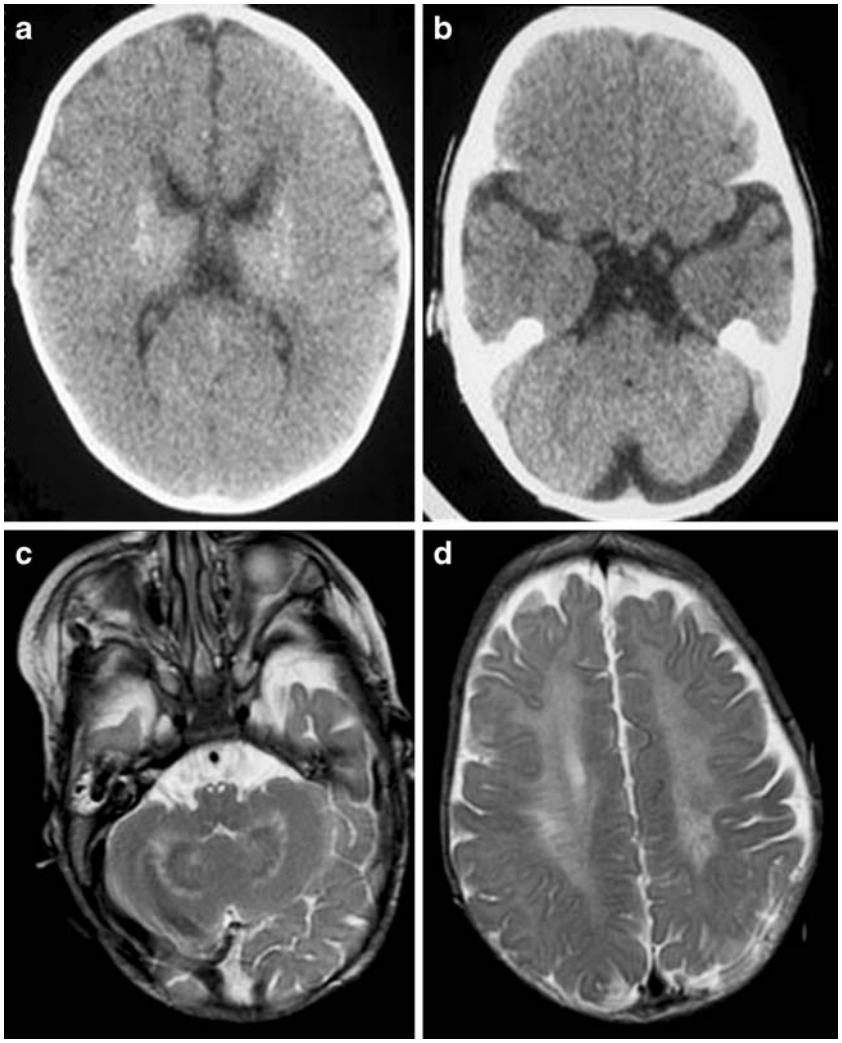

Fig. 13 A 1-year-old boy with Krabbe disease. **a, b** Axial CT images show calcification in the thalami, basal ganglia and dentate. **c** Axial T2-W images confirm abnormality in the dentate with high signal centrally, surrounding low signal and abnormal high signal in peridentate white matter. Abnormal high signal can also be seen in the medial longitudinal fasciculus in the anterior pons. **d** The cerebral deep white matter also has abnormal high signal

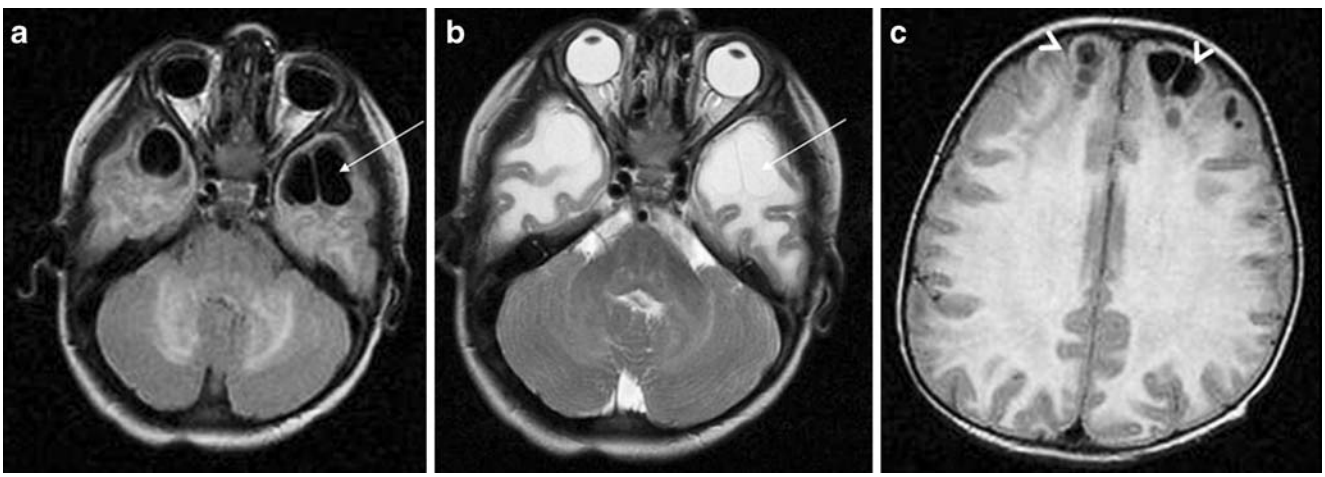

Fig. 14 A 3-year-old child with megalencephalic leukoencephalopathy with cysts. **a** Axial FLAIR and (**b, c**) axial T2-W imaging show (**a, b**) abnormal high signal in the dentate nuclei and swollen white matter with sub-cortical cysts especially in the anterior temporal (*arrows*) and (**c**) frontal lobe white matter (*arrowheads*)

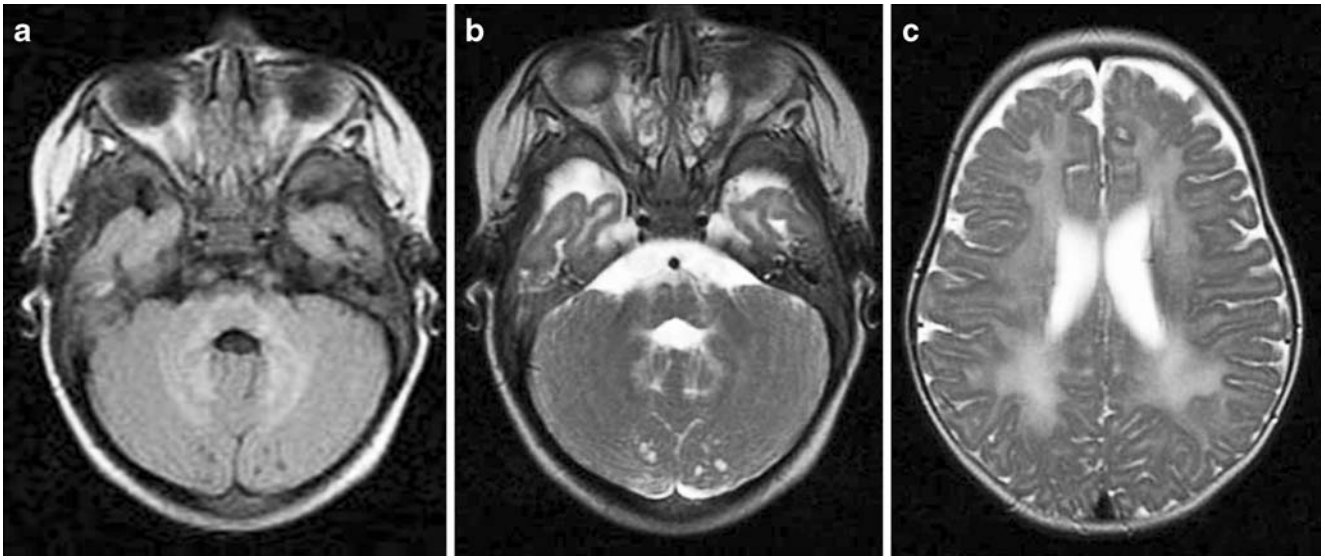

Fig. 15 A 6-month-old girl with merosin negative muscular dystrophy. High signal abnormalities are visible in the dentate nucleus and the pons on (**a**) the T2-W FLAIR and (**b**) T2-W images. **c** Abnormal high T2 signal is also seen in the cerebral deep white matter

been described. In fact a study of 67 patients with crossed cerebellar diaschisis with positron emission tomography (PET) showed glucose metabolism in the contralateral dentate nucleus was relatively preserved [22].

Periventricular leukomalacia (PVL)

We have also noted involvement of the dentate nuclei in PVL. The pathogenesis of PVL, which occurs in pre-term

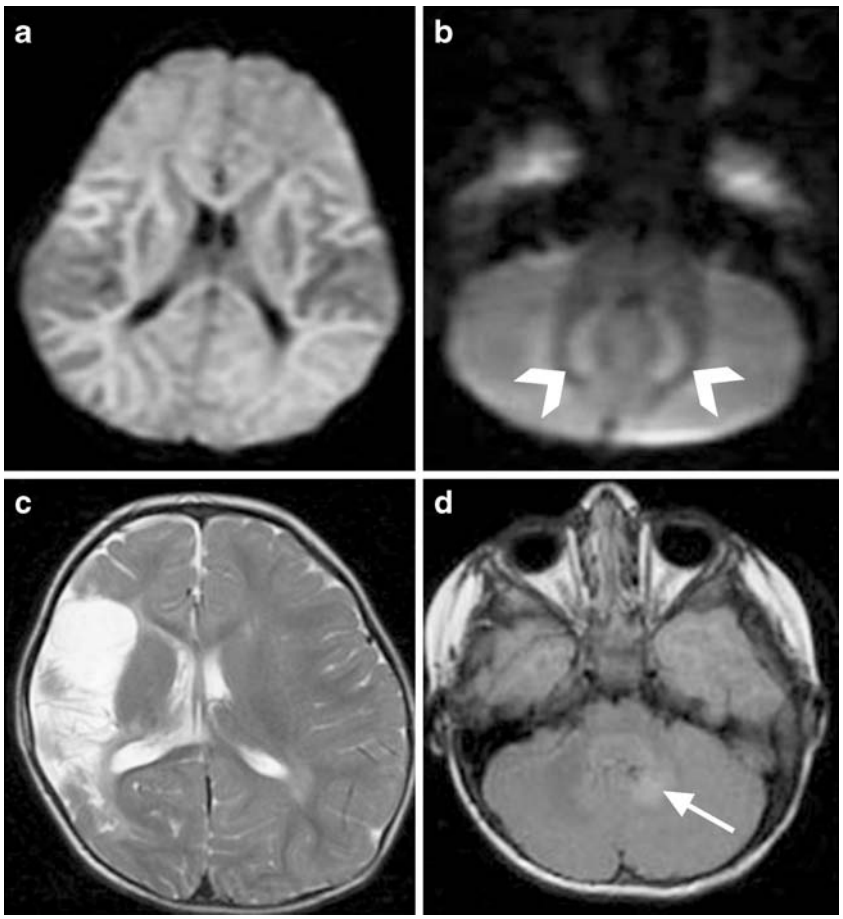

Fig. 16 An 8-month-old girl with severe acute cerebral ischaemia secondary to cardiac arrest. **a** DWI demonstrates diffuse abnormal cerebral diffusion. **b** DWI of the posterior fossa shows markedly abnormal diffusion in both dentate nuclei (*arrowheads*). **c, d** Right middle cerebral artery (MCA) infarction in a 16-month-old girl. On T2-W sequences there is severe cystic encephalomalacia in the right MCA territory. **d**. FLAIR image demonstrates abnormal high signal in the contralateral left dentate nucleus (*arrow*)

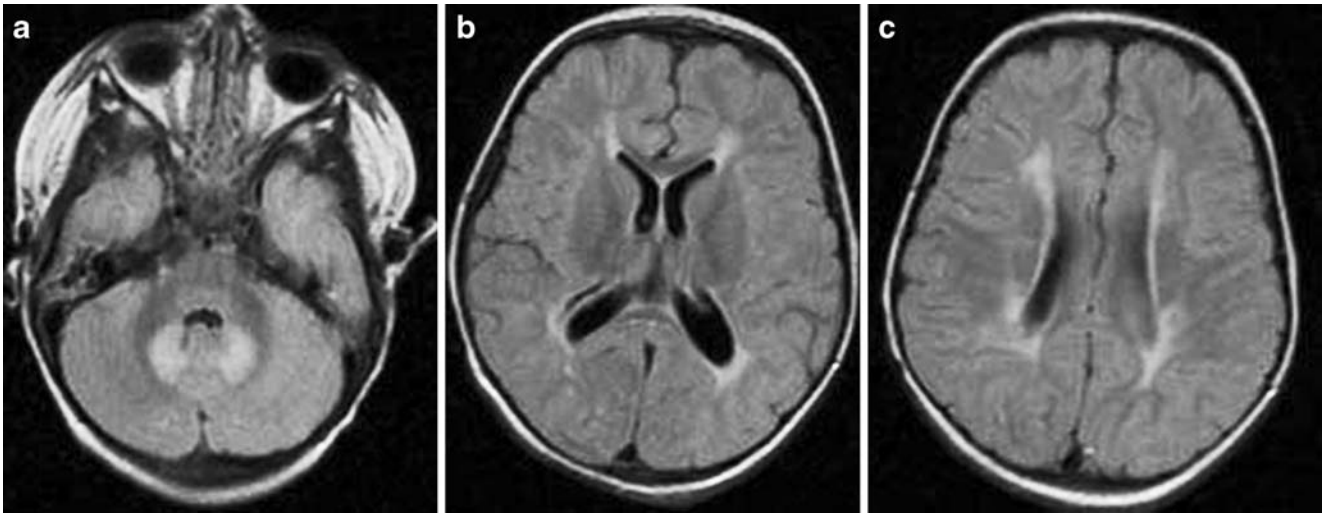

Fig. 17 Axial T2 FLAIR through the posterior fossa, basal ganglia and centrum semi-ovale in a 2-year-old girl with PVL, who was born at 27 weeks' gestation. **a** The dentate nuclei show abnormal high signal. **b, c** Abnormal high signal, cyst formation and volume loss can be seen in the periventricular white matter

infants, was previously believed to be related to ischaemia in watershed zones in the periventricular white matter of immature brains. It is now believed that PVL is probably related to the selective vulnerability of cells of oligodendrocyte lineage to changes of hypoxia-ischaemia.

Early MR changes include abnormal T1 hypointensity and T2 hyperintensity in the periventricular white matter, most frequently in the peritrigonal regions with or without cyst formation [23]. A triad of imaging findings in end-stage PVL include abnormally increased T2 signal and loss of volume in the peritrigonal periventricular white matter bilaterally as well as compensatory focal ventriculomegaly with mild atrial wall irregularity (Fig. 17) [24].

Varicella infection

CNS complications are seen in 1% of cases of childhood varicella zoster infections. These include acute cerebellar ataxia, encephalitis, and vasculitis. In acute cerebellar ataxia MRI reveals diffuse or focal areas of decreased

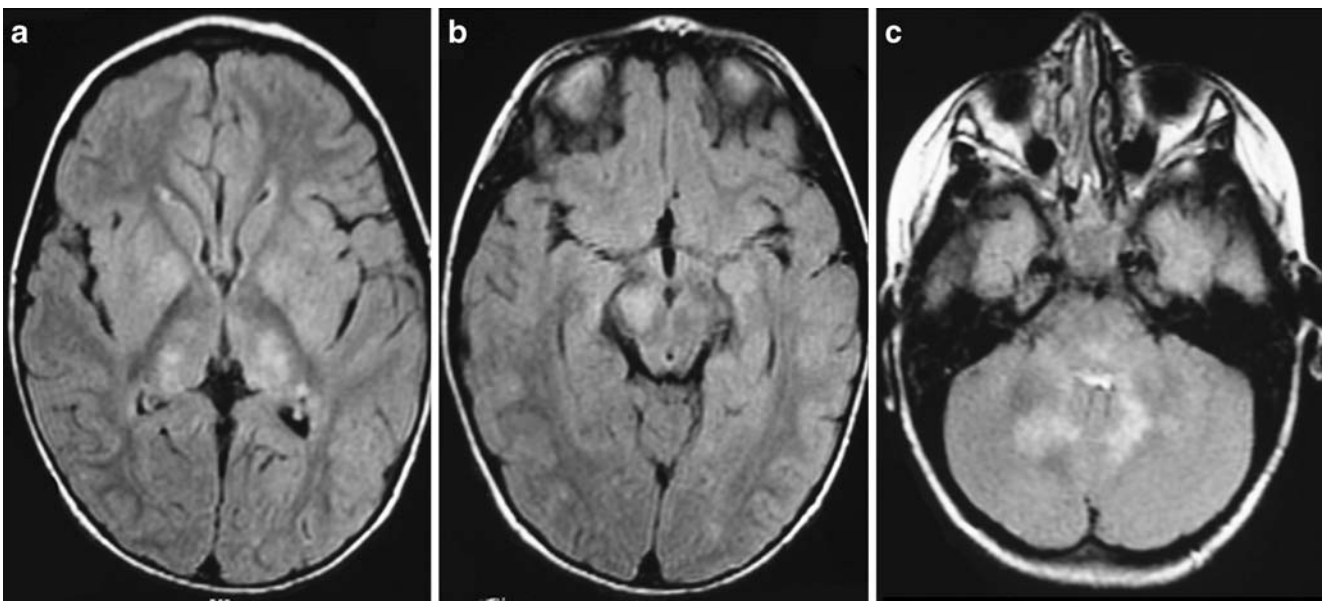

Fig. 18 A 4-year-old girl with varicella zoster infection who presented with encephalitis as the skin lesions were crusting. The encephalitis responded to steroids as expected in ADEM. FLAIR imaging demonstrates abnormal high signal in (**a**) both thalami and lentiform nuclei and (**b**) in right crus cerebri of midbrain. **c** T2-W FLAIR image shows high signal in both dentate nuclei

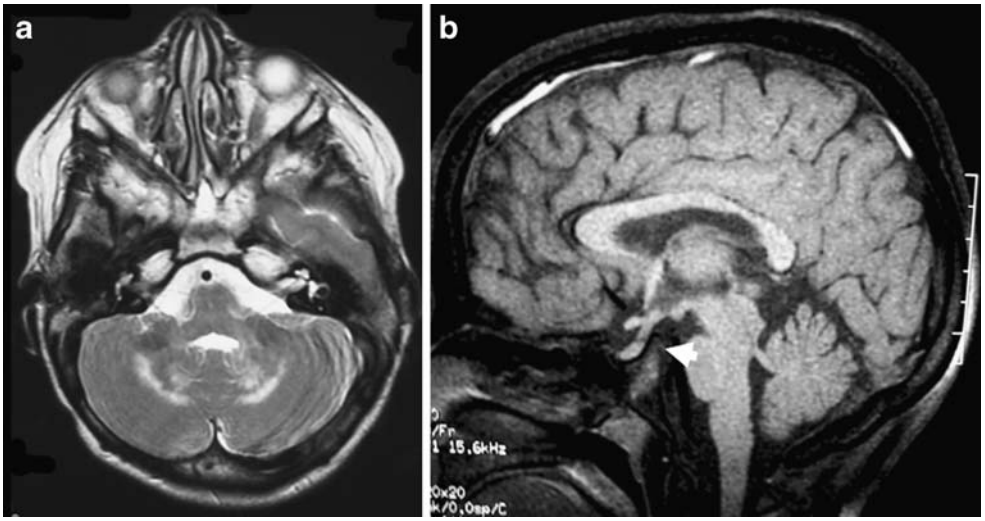

Fig. 19 A 13-year-old girl with LCH. **a** Axial T2-W imaging through the posterior fossa shows high signal in the dentate nuclei bilaterally. **b** Sagittal T1-W image shows absence of the posterior pituitary bright spot (*arrowhead*)

T1- and increased T2-signal in the cerebellum and cerebellar peduncles. The dentate nuclei may be involved. Varicella encephalitis may have a nonspecific pattern similar to other encephalitides, have multifocal cortical and subcortical abnormalities or a clear arterial distribution of abnormal signal. These are all due to varicella vasculitis with different appearances depending on whether small peripheral, medium-size central or larger vessels are affected [25, 26]. Sometimes the encephalitis associated with varicella infection is clinically less severe and is responsive to steroids consistent with an acute disseminated encephalomyelitis (ADEM) and MRI may show multiple supratentorial and infratentorial white matter lesions as well as lesions of the basal ganglia and dentate nuclei (Fig. 18).

Langerhans cell histiocytosis (LCH)

LCH is an aggressive non-neoplastic disorder of unknown aetiology characterised by the intense proliferation of Langerhans cell histiocytes. Diabetes insipidus is a common clinical finding secondary to involvement of the hypothalamus and pituitary infundibulum. Dentate nuclei involvement occurs in up to 40% of patients. Focal T1 hyperintensity in the dentate nuclei can be an early imaging finding with later T2 hyperintensity (Fig. 19) [27, 28].

Neurofibromatosis type 1 (NF1)

NF1 or von Recklinghausen disease is an autosomal-dominant neurocutaneous disorder or phakomatosis. The

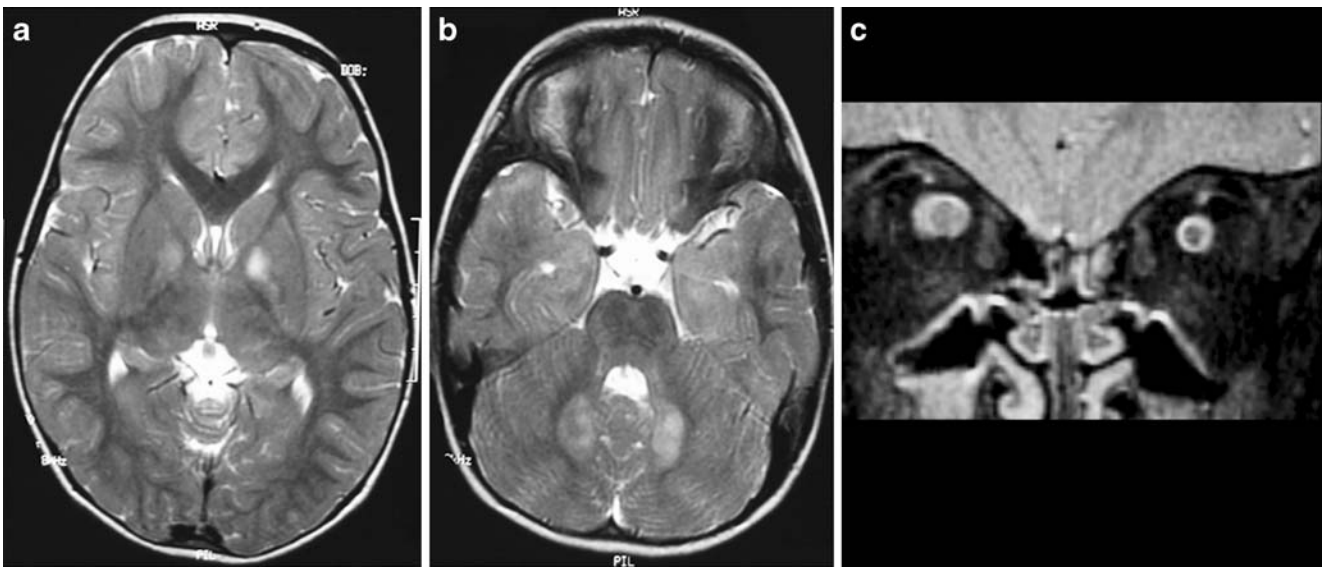

Fig. 20 A 4-year-old boy with NF 1. Axial T2-W images show abnormal hyper-intensity in (**a**) the globus pallidus bilaterally and (**b**) the dentate nuclei characteristic of NBOs. **c** Coronal T2-W fat-saturated image shows diffuse enlargement of the right optic nerve in keeping with an optic nerve glioma

Fig. 21 Disorders associated with dentate nuclei and brain stem abnormalities

Disorders with dentate nuclei and brain-stem involvement	
Metabolic disorders •Maple syrup urine disease •Mitochondrial disorders – Leigh's syndrome •Krabbe disease •Glutaric aciduria – type 1 •Canavan's disease	Miscellaneous disorders •Neurofibromatosis type 1 •Histiocytosis X

hallmark of NF1 is the development of multiple tumours. Characteristic paediatric cerebral imaging findings include neurofibromatosis bright objects (NBO) and optic nerve gliomas (Fig. 20). NBOs are discrete areas of altered signal intensity without mass effect due to foci of myelin vacuolisation. Typical locations include the globus pallidus, cerebellar peduncles, midbrain or pons, internal capsule and splenium of the corpus callosum. Unusual locations include the dentate nucleus and periventricular white matter. Cerebellar white matter and dentate lesions usually occur in children <10 years old and never in the third decade [29]. These areas of myelin vacuolisation are considered benign and most regress or disappear with age [30, 31]. Proliferation and tumour formation in NBOs have been reported

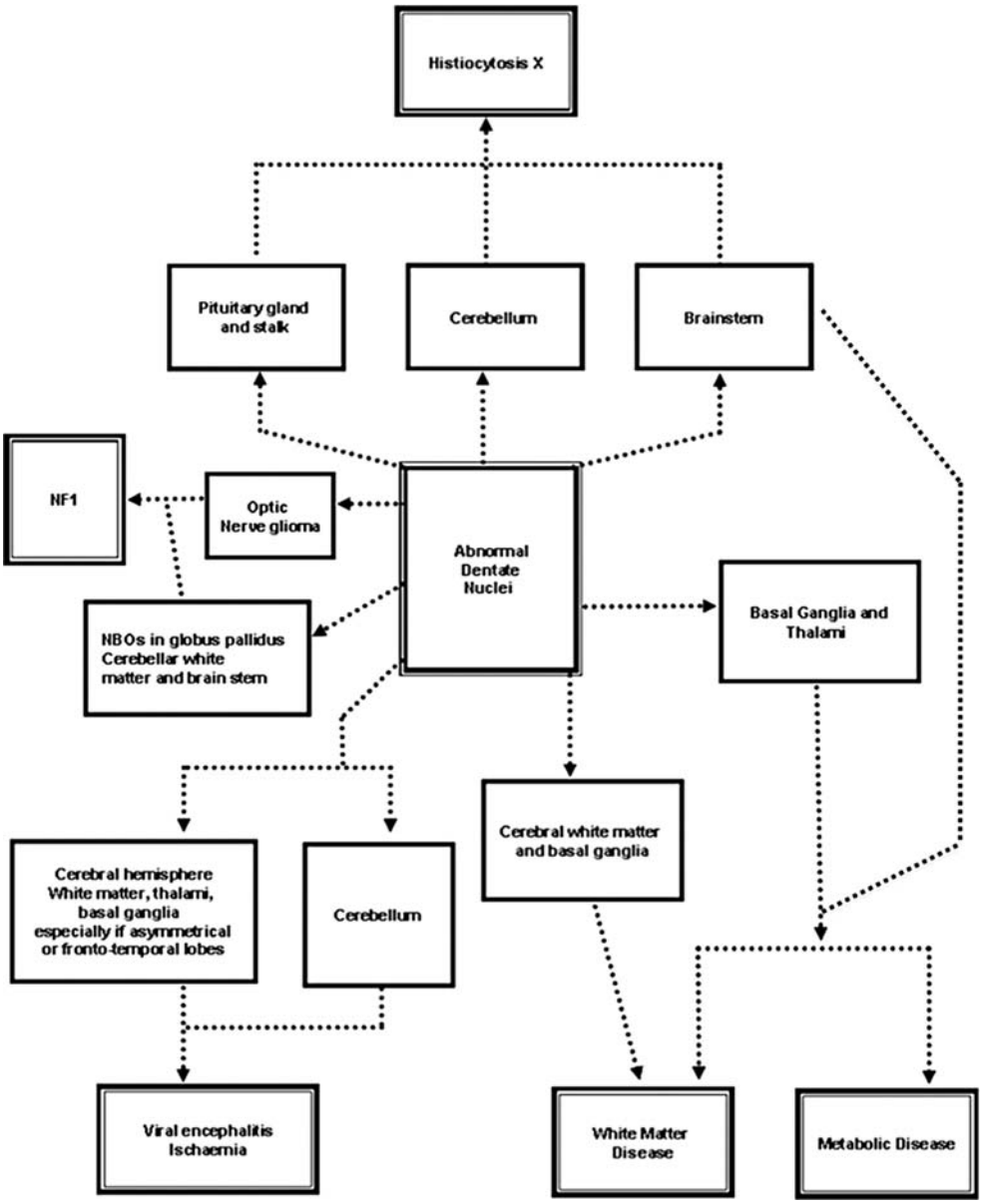

Fig. 22 An approach to dentate nuclei abnormalities identified on MR imaging

especially in those patients with a large number of NBOs. There are however no reported cases of tumour formation in the dentate nuclei [32].

An approach to dentate nuclei abnormalities

Dentate nucleus abnormalities can be seen in a wide spectrum of disease entities. Involvement of the dentate nucleus can be a specific feature in a number of disorders such as organic acidurias (L-2 hydroxyglutaric aciduria and glutaric aciduria type I), infantile Refsum disease, Krabbe disease, LCH and NF1. In other pathological processes the dentate nuclei are infrequently affected or changes are observed only in the later stages of the disease. Concomitant brain stem involvement may also help narrow the differential diagnosis (Fig. 21).

Once the dentate nuclei are deemed abnormal on imaging, a simple schematic approach (Fig. 22) can be used to develop an appropriate differential diagnosis that can act as a guide to clinicians regarding suitable further investigations.

Conclusion

In this article we have reviewed the imaging appearances of normal dentate nuclei as myelination occurs. Armed with this knowledge one is able to more accurately diagnose abnormalities in these deep cerebellar nuclei. As we have demonstrated, a wide variety of pathological processes can affect the dentate nuclei; however, careful assessment of the radiological distribution of disease within the remainder of the brain can help produce a clinically useful differential diagnosis.

References

1. Barkovich AJ (1998) MR of the normal neonatal brain: assessment of deep structures. AJNR 19:1397–1403
2. Kizildag B, Dusunceli E, Fitoz S et al (2005) The role of classic spin echo and FLAIR sequences for the evaluation of myelination in MR imaging. Diagn Interv Radiol 11:130–136
3. Valanne L, Ketonen L, Majander A et al (1998) Neuroradiologic findings in children with mitochondrial disorders. AJNR 19:369–377
4. Hendriksz CJ (2009) Inborn errors of metabolism for the diagnostic radiologist. Pediatr Radiol 39:211–220
5. Finsterer J (2008) Leigh and Leigh-like syndrome in children and adults. Pediatr Neurol 39:223–235
6. Lee HF, Tsai CR, Chi CS et al (2009) Leigh syndrome: clinical and neuroimaging follow-up. Pediatr Neurol 40:88–93
7. Rossi A, Biancheri R, Bruno C et al (2003) Leigh Syndrome with COX Deficiency and SURF-1 gene mutations: MR imaging findings. AJNR 24:1188–1191
8. Twomey EL, Naughten ER, Donoghue VB et al (2003) Neuroimaging findings in glutaric aciduria type 1. Pediatr Radiol 33:823–830
9. Oguz KK, Ozturk A, Cila A (2005) Diffusion-weighted MR imaging and MR spectroscopy in glutaric aciduria type 1. Neuroradiology 47:229–234
10. Takanashi J, Fujii K, Sugita K et al (1999) Neuroradiologic findings in glutaric aciduria type II. Pediatr Neurol 20:142–145
11. Topçu M, Erdem G, Saatçi I et al (1996) Clinical and magnetic resonance imaging features of L-2-hydroxyglutaric acidemia: report of three cases in comparison with Canavan disease. J Child Neurol 11:373–377
12. Kara S, Sherr EH, Barkovich AJ (2008) Dilated perivascular spaces: an informative radiologic finding in Sanfilippo syndrome type A. Pediatr Neurol 38:363–366
13. Aicardi J, Goutières F (1984) A progressive familial encephalopathy in infancy with calcifications of the basal ganglia and chronic cerebrospinal fluid lymphocytosis. Ann Neurol 15:49–54
14. Uggetti C, La Piana R, Orcesi S et al (2009) Aicardi-Goutières syndrome: neuroradiologic findings and follow-up. AJNR 30:1971–1976
15. Choksi V, Hoeffner E, Karaarslan E et al (2003) Infantile Refsum disease: case report. AJNR 24:2082–2084
16. Di Rocco M, Biancheri R, Rossi A et al (2004) MRI in acute intermittent maple syrup urine disease. Neurology 63:1078
17. Patay Z (2005) Diffusion-weighted MR imaging in leukodystrophies. Eur Radiol 15:2284–2303
18. Provenzale JM, Peddi S, Kurtzberg J et al (2009) Correlation of neurodevelopmental features and MRI findings in infantile Krabbe's disease. AJR 192:59–65
19. Nagar VA, Ursekar MA, Krishnan P et al (2006) Krabbe disease: unusual MRI findings. Pediatr Radiol 36:61–64
20. Sener RN (2000) van der Knapp syndrome: MR imaging findings including FLAIR, diffusion imaging and proton MR spectroscopy. Eur Radiol 10:1452–1455
21. van der Knaap MS, Smit LM, Barth PG et al (1997) Magnetic resonance imaging in classification of congenital muscular dystrophies with brain abnormalities. Ann Neurol 42:50–59
22. Fulham MJ, Brooks RA, Hallett M et al (1992) Cerebellar diaschisis revisited: pontine hypometabolism and dentate sparing. Neurology 42:2267–2273
23. Huang BY, Castillo M (2008) Hypoxic-ischemic brain injury: imaging findings from birth to adulthood. Radiographics 28:417–439
24. Baker LL, Stevenson DK, Enzmann DR (1988) End-stage periventricular leucomalacia: MR evaluation. Radiology 168:809–815
25. Baskin HJ, Hedlund G (2007) Neuroimaging of herpes infections in children. Pediatr Radiol 37:949–963
26. Montenegro MA, Santos SL, Li LM et al (2002) Neuroimaging of acute cerebellitis. J Neuroimaging 12:72–74
27. Prayer D, Grois N, Prosch H et al (2004) MR imaging presentation of intracranial disease associated with Langerhans cell histiocytosis. AJNR 25:880–891
28. Martin-Duverneuil N, Idbaih A, Hoang-Xuan K et al (2006) MRI features of neurodegenerative Langerhans cell histiocytosis. Eur Radiol 16:2074–2082
29. Itoh T, Magnaldi S, White RM et al (1994) Neurofibromatosis type 1: the evolution of deep gray and white matter MR abnormalities. AJNR 15:1513–1519
30. Herron J, Darrah R, Quaghebeur G (2000) Intra-cranial manifestations of neurocutaneous syndromes. Clin Radiol 55:82–98
31. Jacques C, Dietemann JL (2005) Imaging features of neurofibromatosis type 1. Neuroradiology 32:180–197
32. Griffiths PD, Blaser S, Mukonoweshuro W et al (1999) Neurofibromatosis bright objects in children with Neurofibromatosis type 1: a proliferative potential? Pediatrics 104:e49